ACCEPTED FOR PUBLICATION IN ApJ
Preprint typeset using LATEX style emulateapj v. 10/09/06

DO BROAD ABSORPTION LINE QUASARS LIVE IN DIFFERENT ENVIRONMENTS FROM ORDINARY QUASARS?

YUE SHEN[1], MICHAEL A. STRAUSS[1], PATRICK B. HALL[2], DONALD P. SCHNEIDER[3], DONALD G. YORK[4], NETA A. BAHCALL[1]

accepted for publication in ApJ

ABSTRACT

We select a sample of ~ 4200 traditionally defined broad absorption line quasars (BALQs) from the Fifth Data Release quasar catalog of the Sloan Digital Sky Survey. For a statistically homogeneous quasar sample with $1.7 \leq z \leq 4.2$, the BAL quasar fraction is $\sim 14\%$ and is almost constant with redshift. We measure the auto-correlation of non-BAL quasars (nonBALQs) and the cross-correlation of BALQs with nonBALQs using this statistically homogeneous sample, both in redshift space and using the projected correlation function. We find no significant difference between the clustering strengths of BALQs and nonBALQs. Assuming a power-law model for the real space correlation function $\xi(r) = (r/r_0)^{-1.8}$, the correlation length for nonBALQs is $r_0 = 7.6 \pm 0.8\, h^{-1}$Mpc; for BALQs, the cross-correlation length is $r_0 = 7.4 \pm 1.1\, h^{-1}$Mpc. Our clustering results suggest that BALQs live in similar large-scale environments as do nonBALQs.

Subject headings: galaxies: active – quasars: absorption lines – quasars: emission lines – quasars: general

1. INTRODUCTION

Broad absorption line (BAL) quasars constitute a significant fraction, $\sim 10-20\%$ of the entire quasar population (Weymann 2002; Tolea et al. 2002; Hewett & Foltz 2003; Reichard et al. 2003a; Trump et al. 2006). While the broad absorption features are usually explained by invoking an outflowing wind, it remains unclear how special BAL outflows are. Is it that $\sim 10-20\%$ of the whole quasar population has such BAL outflows, or do most quasars have BAL outflows, but with an average wind covering fraction of $\sim 10-20\%$? The former case would suggest that BALQs are an intrinsically physically distinct class of quasars, while the latter model implies that the BAL phenomenon is an accident of orientation. Current observations are consistent with most BALQs being intrinsically no different from ordinary quasars, with the BAL phenomenon arising when the line-of-sight cuts through low covering fraction outflows, as produced in some disk wind models (e.g., Murray et al. 1995; Proga et al. 2000; Elvis 2000 and references therein). Spectropolarimetry shows that there are absorption-line-free lines of sight in BAL quasars, and the wind covering fraction is inferred to be low from constraints on ultraviolet emission-line scattering (e.g., Hamann et al. 1993; Ogle et al. 1999; but cf. Brotherton et al. 2006). The continuum and emission line properties of BALQs suggest a disk wind/orientational-obscuration geometry (e.g., Reichard et al. 2003a,b). Gallagher et al. (2007) found no compelling evidence for inherent differences in composite mid-infrared through X-ray SEDs between BAL and non-BAL quasars of comparable luminosity. Shen et al. (2007b) found that the distribution of black hole masses measured from the Mg II virial estimator is almost identical between a C IV BAL and a non-BAL quasar sample matched in redshift and luminosity, similar to what was found in Ganguly et al. (2007).

Of course, there are still many unsettled issues regarding BALQs. For example, the exact geometry of these outflows is still under theoretical investigation (e.g., Proga 2007) and observational debate. It has been argued based on the properties of radio-loud BAL quasars (Becker et al. 2000, and references therein) that the outflow cannot be purely equatorial in at least some cases. For example, Brotherton et al. (2006) reported a radio-loud BAL quasar whose spectropolarimetry is consistent with it being viewed closer to pole-on than edge-on. Based on radio variability arguments which yield high brightness temperatures, Zhou et al. (2006) and Ghosh & Punsly (2007) argue that some BAL quasars are viewed nearly along the polar axis (but see Blundell & Kuncic 2007). However, the exact geometry of BAL outflows is immaterial when considering whether or not BAL quasars form a distinct subpopulation of quasars.

A somewhat different test of whether BALQs are a distinct quasar subpopulation is to search for differences in their large-scale environments as probed by their clustering properties. Since quasars live in dark matter halos, and more massive dark matter halos are more highly biased and therefore have intrinsically stronger spatial clustering, the clustering properties of quasars can constrain the masses of their host dark matter halos (Shen et al. 2007a and references therein). A difference in the clustering properties between BALQs and nonBALQs will directly imply BALQs belong to a distinct class, hence such a test is crucial to the current BAL quasar picture. However, such analyses require large and statistically homogeneous BAL quasar samples, and were thus impractical in earlier studies on BALQs (e.g., Weymann et al. 1991; Hewett & Foltz 2003). The Sloan Digital Sky Survey (SDSS, York et al. 2000) has made such studies possible by providing a large sample of optically-selected quasars (see Schneider et al. 2007 for the latest SDSS quasar catalog), from which we can construct homogeneous subsamples for clustering studies. BAL quasar catalogs constructed using SDSS quasars have greatly increased the number of BALQs known in the literature. The latest SDSS BAL quasar catalog, based on Data Release Three (Abazajian et al. 2005), was compiled by Trump et al. (2006) and contains ~ 2000 traditional BALQs.

In this paper, we extend the traditional BAL quasar catalog to the fifth SDSS data release (DR5, Adelman-McCarthy et al. 2007), and investigate the clustering properties of BALQs

[1] Princeton University Observatory, Princeton, NJ 08544.
[2] Dept. of Physics & Astronomy, York University, 4700 Keele St., Toronto, ON, M3J 1P3, Canada.
[3] Department of Astronomy and Astrophysics, 525 Davey Laboratory, Pennsylvania State University, University Park, PA 16802.
[4] University of Chicago and Enrico Fermi Institute, 5640 So. Ellis Avenue, Chicago, IL 60637

based on statistically homogeneous samples. We describe the construction of our BAL quasar samples in §2, present the clustering measurements in §3 and discuss our results in §4. Throughout this paper we adopt a flat ΛCDM cosmology: $\Omega_M = 0.26$, $\Omega_\Lambda = 0.74$ and $h = 0.71$ (Spergel et al. 2007).

2. SAMPLE SELECTION

Our parent sample is the published DR5 quasar catalog (Schneider et al. 2007), which contains 77,429 quasars. About half the quasars in this catalog were targeted using a uniform algorithm (Richards et al. 2002) and will be used to construct statistically homogeneous subsamples for our clustering analysis (e.g., Richards et al. 2006; Shen et al. 2007a).

BALQs are identified using the traditional "Balnicity Index" (BI) criterion (Weymann et al. 1991, see the definition in their Appendix A). Our procedure is similar to Reichard et al. (2003a) and Trump et al. (2006): the input spectrum is fitted by a composite quasar spectrum with adjustable power-law scaling and dust reddening, normalized using different continuum windows (see section 3.3 in Reichard et al. 2003a for details). We have used the Vanden Berk et al. (2001) composite quasar spectrum constructed from the SDSS Early Data Release (EDR, Stoughton et al. 2002), and the Pei (1992) SMC extinction curve (e.g., Hopkins et al. 2004). The continuum normalization windows are 1725 ± 25 Å for CIV and 3150 ± 25 Å ($0.5 \leq z \leq 1.9$) and 2200 ± 25 Å ($1.9 < z \leq 2.1$) for MgII . Once we have the composite fits, BALQs are identified for quasars with CIV absorption at least 2000 km s^{-1} broad located between 3000 and 25,000 km s^{-1} blueward of the quasar redshift; or with MgII absorption at least 1000 km s^{-1} broad located between 0 and 25,000 km s^{-1} blueward of the quasar redshift. Thus given the SDSS spectral coverage, complete BAL quasar samples can only be identified within $1.7 \leq z \leq 4.2$ for CIV and $0.5 \leq z \leq 2.1$ for MgII , and so we restrict ourselves to these redshift ranges.

The procedure we describe in this paper is not identical to that of Trump et al. (2006). In particular, when measuring absorption troughs we have boxcar smoothed the input spectrum by 15 pixels, while Trump et al. used a smoothing window of three pixels. This increases our sensitivity to weak BAL features but also greatly increases the rate of false detections. Also, we are using the Vanden Berk et al. (2001) composite spectrum for all input spectra, instead of using different templates as Trump et al. (2006) did, which allow for variations in emission-line strength and shape.

Although automatic pipelines are efficient for large samples, there will inevitably be false and missing identifications. For this reason, we examined the spectra of the entire DR5 quasar catalog by eye, and moved objects into or out of the BAL quasar catalog. We found that out automated procedure missed only about 1% of BALQs in our final sample; while the false detection rate is quite high (over half are actually quasars with high velocity narrow absorption lines), primarily caused by the 15-pixel boxcar smoothing. Therefore our manual inspection is necessary to include only BALQs in our sample. In comparison to the DR3 portion in the Trump et al. (2006) catalog, some weak BALQs are not included in our catalog, while we also include some strong BALQs that are apparently missing in the Trump et al. catalog. Ganguly et al. (2007) manually inspected the Trump et al. catalog, and also concluded that automatic ID procedures are not perfect. Our final catalog contains 4203 BALQs. This list is perhaps still incomplete to some extent, and less restrictive BAL criteria such as the AI index (Hall et al. 2002) used in the Trump et al. catalog will certainly increase the number of BALQs. The distribution of the CIV balnicity index is similar to what was found by Tolea et al. (2002) and Reichard et al. (2003a), with more BALQs at the lower BI end. But determining the exact distribution of the BI index will require more careful work on individual spectral fits, which we defer to a BAL quasar catalog paper in preparation.

Quasars showing MgII BAL almost always show CIV BAL as well, but the reverse is not true. Hence our BAL quasar catalog is close to complete for $1.7 \leq z \leq 4.2$, where the spectral coverage allows us to identify CIV BALQs. We now further restrict ourselves to uniformly-selected quasars based on color-selection (Richards et al. 2002). These uniformly-targeted quasars are flux limited to $i = 19.1$ at $z \lesssim 3$ and $i = 20.2$ at $z \gtrsim 3$, [5] and are selected using the final quasar target algorithm (see details in Richards et al. 2002) implemented after DR1 (Abazajian et al. 2003). This results in statistically homogeneous samples of 12,117 nonBALQs and 1942 BALQs in the redshift range $1.7 \leq z \leq 4.2$. The distributions of these nonBALQs and BALQs in the redshift-luminosity diagram are shown in Fig. 1 as gray and black dots respectively. Their distributions are almost indistinguishable, and the BAL quasar fraction[6], $\sim 14\%$, is nearly constant with redshift. There is an apparent excess of BALQs at $z \sim 2.7$. This is because around this redshift the colors of quasars are similar to those of F stars (Fan 1999) and the quasar target selection becomes less efficient; BALQs have different broad band colors and are perhaps less sensitive to this selection inefficiency. Despite this detail, there is little evidence that the BAL quasar fraction changes significantly within this redshift range. We take these uniformly-selected subsamples as our clustering subsamples. Given the similarity in the redshift and luminosity distributions of BALQs and nonBALQs in these subsamples, we can fairly compare the difference, if there is any, in the clustering properties of BALQs and nonBALQs.

The complete list of BALQs and nonBALQs with flags indicating whether or not each is included in the clustering analysis is presented in Table 1 of Shen et al. (2007b).

3. CLUSTERING ANALYSIS

Following Shen et al. (2007a), we generate random catalogs according to the detailed angular and radial geometries of our clustering subsamples. We measure the auto-correlation of nonBALQs, and the cross-correlation of nonBALQs around BALQs. Our BAL quasar sample is quite sparse, and therefore its auto-correlation function is too noisy to be useful. We use the cross-correlation technique to boost the clustering signal and to achieve reasonable measurements. While it is straightforward to measure the redshift space correlation function $\xi_s(s)$, such measurements suffer from redshift distortions and the uncertainties in redshift determinations. Using the projected correlation function $w_p(r_p)$ avoids these problems (e.g., Davis & Peebles 1983), and gives an unbiased estimate of the real space correlation function $\xi(r)$. In estimating errors, we use jackknife resampling following Shen et al. (2007a).

[5] There are a few $i > 19.1$ quasars at $z \lesssim 3$ which were selected by the high-z (*griz*) branch of the targeting algorithm (Richards et al. 2002). The fraction of these objects is tiny ($\lesssim 2\%$) and does not affect our analysis.

[6] The BAL quasar fraction here is the raw fraction, i.e., without corrections for intrinsic extinction. Dai et al. (2007) recently measured an intrinsic BAL fraction (using the traditional BI definition) of $\sim 20\%$ based on a sample of 2MASS (Skrutskie et al. 2006) matched SDSS quasars (see also Hewett & Foltz 2003).

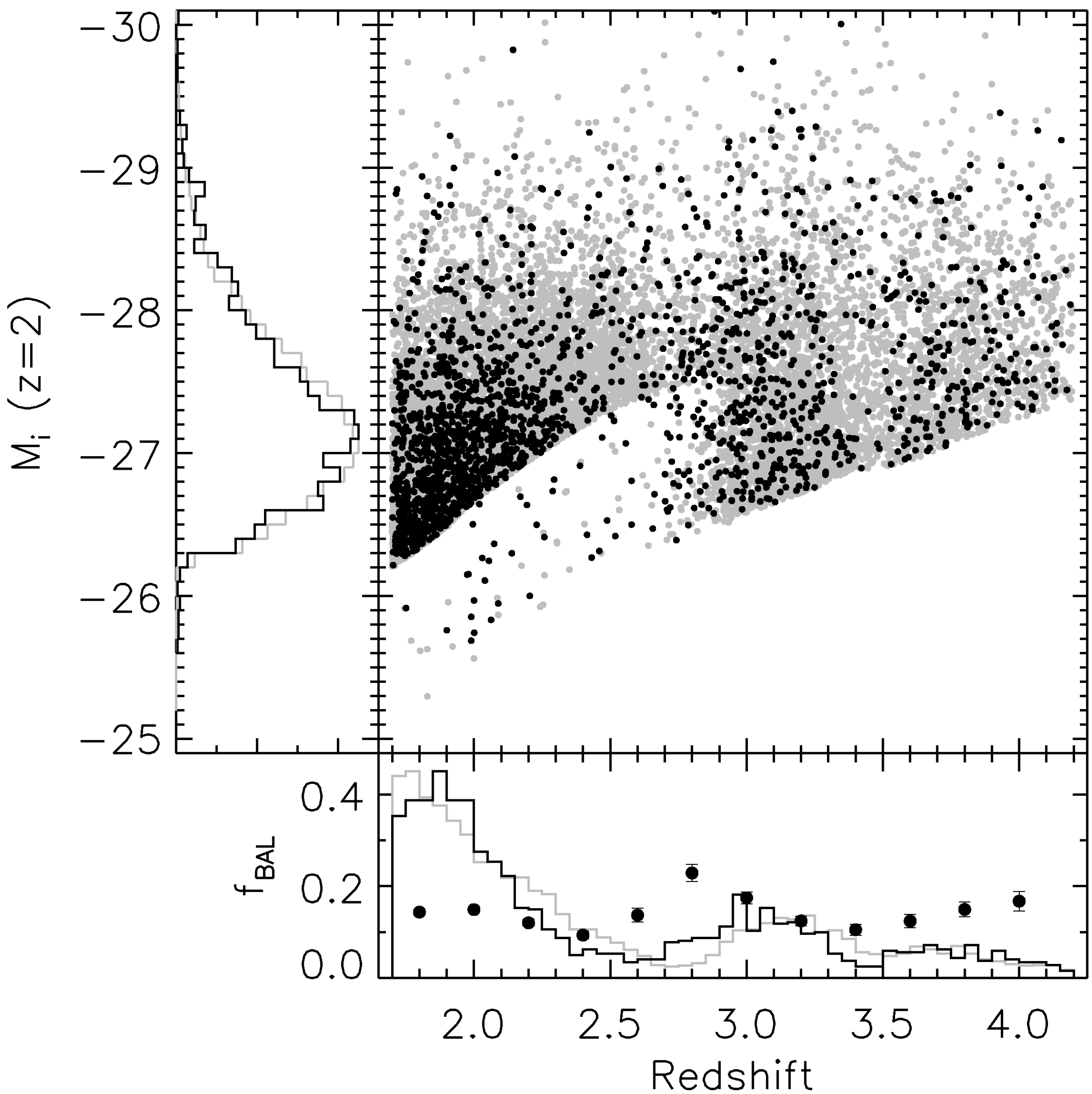

FIG. 1.— Distribution of our statistically homogeneous samples of CIV BALQs (black dots) and nonBALQs (gray dots) in the redshift-luminosity plane. The left and bottom panels show the histograms of i–band absolute magnitudes (K–corrected to $z = 2$, Richards et al. 2006) and redshifts, gray for nonBALQs and black for BALQs. In the bottom panel we also show the BAL quasar fraction (with statistical errors) as function of redshift in filled circles. Despite the jump around $z \sim 2.7$, which may be caused by the general inefficiency in color selection around this redshift (see text), the BAL quasar fraction $\sim 14\%$ is almost constant with redshift.

For the auto-correlation function of nonBALQs, we use the Landy & Szalay (1993) estimator:

$$\xi_s(s),\ \xi_s(r_p,\pi) = \frac{\langle DD\rangle - 2\langle DR\rangle + \langle RR\rangle}{\langle RR\rangle}\ , \quad (1)$$

where $\langle DD\rangle$, $\langle DR\rangle$, and $\langle RR\rangle$ are the normalized numbers of data-data, data-random and random-random pairs, respectively, in our desired bins. The projected correlation function is then obtained by integrating the two-dimensional redshift space correlation function $\xi_s(r_p,\pi)$ along the line-of-sight (π) direction:

$$w_p(r_p) = 2\int_0^\infty d\pi\, \xi_s(r_p,\pi)\ . \quad (2)$$

In practice we cut this integral at $\pi_{\rm cutoff} = 50\ h^{-1}$Mpc. We find $\pi_{\rm cutoff} = 70\ h^{-1}$Mpc and $100\ h^{-1}$Mpc give essentially identical results, but with larger uncertainties since more noise is added.

For the cross-correlation of nonBALQs around BALQs, we use the estimator (e.g., Coil et al. 2007)

$$\xi_s(s),\ \xi_s(r_p,\pi) = \frac{\langle BN\rangle}{\langle BR\rangle} - 1\ , \quad (3)$$

where $\langle BN\rangle$ and $\langle BR\rangle$ are normalized BAL-nonBAL quasar and BAL quasar-random pairs at a given separation. To compute the projected cross-correlation function, we again use $\pi_{\rm cutoff} = 50\ h^{-1}$Mpc.

Our results are shown in Fig. 2 for the redshift space correlation function (left) and projected correlation function (right), along with fitted power-law models. For the redshift space correlation function, the fitted power-law $\xi_s(s) = (s/s_0)^{-\delta}$ has $s_0 = 8.6 \pm 1.3\ h^{-1}$Mpc, $\delta = 1.5 \pm 0.2$ for nonBALQs for the fitting range $4 < s < 150\ h^{-1}$Mpc; $s_0 = 7.3 \pm 1.3\ h^{-1}$Mpc or $9.7 \pm 1.3\ h^{-1}$Mpc for the nonBAL-BAL quasar cross correlation when we include all the data points or exclude the two negative points at $s \approx 15$ and $55\ h^{-1}$Mpc respectively, for the same fitting range $4 < s < 150\ h^{-1}$Mpc and fix-

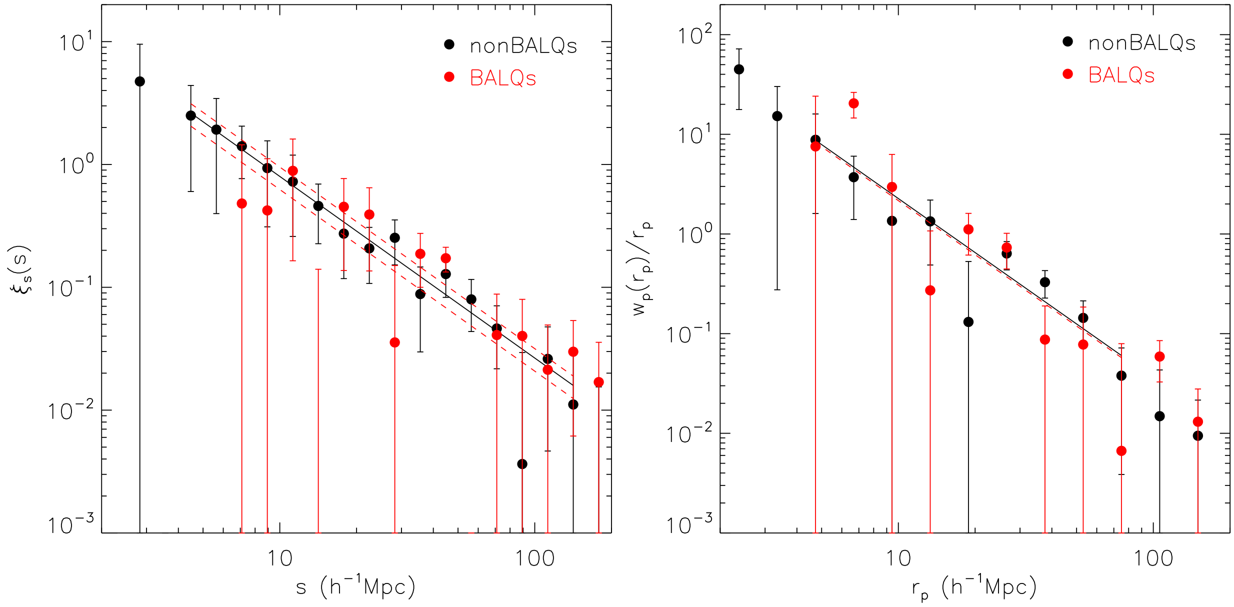

FIG. 2.— Redshift space (left) and projected (right) correlation functions. Black and red colors denote the nonBAL quasar auto-correlation and the BAL-nonBAL quasar cross-correlation, respectively. Errors are estimated using the jackknife method. The solid and dashed lines are fitted power-law models. The fitting ranges are $4 < s < 150\ h^{-1}$Mpc for the redshift space correlation function, and $4 < r_p < 80\ h^{-1}$Mpc for the projected correlation function. The upper and lower dashed lines in the left panel are two fits to the BAL-nonBAL quasar cross correlation, including and excluding the two negative data points at $s \approx 15$ and $55\ h^{-1}$Mpc.

ing the power-law slope to be the same as the nonBAL quasar case. For the projected correlation function and assuming a power-law real space correlation function $\xi(r) = (r/r_0)^{-1.8}$ we have: $r_0 = 7.6 \pm 0.8\ h^{-1}$Mpc and $r_0 = 7.4 \pm 1.1\ h^{-1}$Mpc for the nonBAL quasar and cross-correlation cases respectively, for the fitting range $4 < r_p < 80\ h^{-1}$Mpc. Although the data points scatter around these fitted power-law models (especially for the nonBAL-BAL quasar cross correlation), and the jackknife error estimator might be inadequate for sparse samples, we find no convincing evidence that the auto-correlation function of nonBALQs is different from their cross-correlation function with BALQs. Hence our results suggest that BALQs and nonBALQs live in similar environments on large scales, and therefore lie in similar dark matter halos.

The quasar correlation function evolves with redshift, especially for $z \gtrsim 2.8$ (Shen et al. 2007a). Hence we divide our sample into two redshift bins, $1.7 \leq z \leq 2.8$ and $2.8 \leq z \leq 4.2$, and repeat the clustering analysis. We still did not find any compelling difference between the auto-correlation function of nonBALQs and the cross-correlation function of nonBALQs-BALQs within each redshift bin, although the cross-correlation function is quite noisy for the higher redshift bin due to the smaller numbers of both non-BALQs and BALQs.

A potential drawback of our analysis is that the velocity width cut (2000 km s^{-1} for C IV) used in the BI definition of a BAL quasar is rather arbitrary. By imposing such a cut we are rejecting high-velocity narrow absorption line (NAL) quasars into the "nonBAL" quasar sample. The fraction of these NAL quasars to the entire population is perhaps $\gtrsim 10\%$ based on the excess fraction of BALQs selected using the AI definition (which loosens the velocity width cut to be 1000 km s^{-1}) in the Trump et al. catalog. In addition, $\sim 25\%$ of all quasars show associated absorption line (AAL) systems (e.g., Ganguly et al. 2001; Vestergaard 2003; Ganguly & Brotherton 2007), which are not included in our BI based BAL quasar sample. NAL and AAL quasars together make up $\sim 37\%$ of the entire quasar population and $\sim 40\%$ of our nonBAL quasar sample based on the estimations by Ganguly et al. (2007). Of course, not all of these NAL and AAL systems are intrinsically associated with the quasar; some must be intervening systems. If those intrinsic NAL and AAL systems[7] have the same clustering as BALQs but have different clustering from absorption-free quasars, then including them in our nonBAL quasar clustering subsample would potentially dilute any possible difference in clustering between BAL/NAL/AAL quasars and absorption-free quasars. To test this, we have selected a "cleaned" sample of ~ 8000 absorption-free quasars from our nonBAL quasar clustering subsample, and measured their auto-correlation function. Although the signal-to-noise ratio is lower, we found no convincing difference from using the whole nonBAL quasar sample, reassuring that we are not biasing our results. This result is also consistent with the general picture that quasar outflows are ubiquitous, while the modest covering factor of these various (BAL or NAL) outflows causes the different appearances of quasars with and without absorption features.

4. DISCUSSION

We have made the first attempt to measure the clustering properties of broad absorption quasars, based on the largest and most homogeneous BAL quasar sample available. However, the sparseness of the BAL quasar sample (~ 0.5 per deg^2 over a wide redshift range) prohibits direct measurement of the BAL quasar auto-correlation function. To boost the clustering signal, we have cross-correlated BALQs with the ~ 6 times larger sample of nonBALQs at the same redshifts. Our results suggest that BALQs have similar clustering properties as nonBALQs on the scales probed by our sample, and hence

[7] A recent study on ~ 400 MgII AAL systems suggests that the absorption originates from gas in the host galaxies of quasars (e.g., Vanden Berk et al., 2007), suggesting that they would have the same clustering properties as ordinary quasars. A clustering analysis of AAL systems using a large sample from SDSS DR5 is underway to test this hypothesis.

should reside in similar large-scale environments.

Our clustering results provide support to the idea that BALQs are drawn uniformly from the overall underlying population of quasars, as would be the case if (for example) BAL troughs arose in disk wind outflows (Murray et al. 1995; Proga et al. 2000; Elvis 2000). The nearly constant BAL quasar fraction with redshift in our optical quasar sample is also consistent with this picture. It may still be that members of the rare subclass of FeLoBALQs are intrinsically different from ordinary quasars (Farrah et al. 2007), and may reside in different environments. Unfortunately, the small number of FeLoBALQs in our sample makes a clustering analysis of them too noisy to be useful.

We thank Linhua Jiang for pointing out some missing objects in our original BAL quasar sample and Jenny Greene for helpful discussions. YS and MAS acknowledge the support of NSF grants AST-0307409 and AST-0707266. PBH is supported by NSERC. DPS acknowledges the support of NSF grant AST-0607634.

Funding for the SDSS and SDSS-II has been provided by the Alfred P. Sloan Foundation, the Participating Institutions, the National Science Foundation, the U.S. Department of Energy, the National Aeronautics and Space Administration, the Japanese Monbukagakusho, the Max Planck Society, and the Higher Education Funding Council for England. The SDSS Web Site is http://www.sdss.org/.

The SDSS is managed by the Astrophysical Research Consortium for the Participating Institutions. The Participating Institutions are the American Museum of Natural History, Astrophysical Institute Potsdam, University of Basel, University of Cambridge, Case Western Reserve University, University of Chicago, Drexel University, Fermilab, the Institute for Advanced Study, the Japan Participation Group, Johns Hopkins University, the Joint Institute for Nuclear Astrophysics, the Kavli Institute for Particle Astrophysics and Cosmology, the Korean Scientist Group, the Chinese Academy of Sciences (LAMOST), Los Alamos National Laboratory, the Max-Planck-Institute for Astronomy (MPIA), the Max-Planck-Institute for Astrophysics (MPA), New Mexico State University, Ohio State University, University of Pittsburgh, University of Portsmouth, Princeton University, the United States Naval Observatory, and the University of Washington.

Facilities: Sloan

REFERENCES

Abazajian, K., et al. 2003, AJ, 126, 2081 (DR1)
Abazajian, K., et al. 2005, AJ, 129, 1755 (DR3)
Adelman-McCarthy, J. K., et al. 2007, ApJS, 172, 634 (DR5)
Becker, R. H., et al. 2000, ApJ, 538, 72
Blundell, K. M., & Kuncic, Z. 2007, ApJ, 668, L103
Brotherton, M. S., De Breuck, C., & Schaefer, J. J. 2006, MNRAS, 372, L58
Coil, A., Hennawi, J. F., Newman, J. A., Cooper, M. C., & Davis, M. 2007, ApJ, 654, 115
Dai, X., Shankar, F., & Sivakoff, G. R. 2007, ApJ, in press, arXiv: 0704.2882
Davis, M., & Peebles, P. J. E. 1983, ApJ, 267, 465
Elvis, M. 2000, ApJ, 545, 63
Fan, X. 1999, AJ, 117, 2528
Farrah, D., Lacy, M., Priddey, R., Borys, C., & Alfonso, J. 2007, ApJ, 662, L59
Gallagher, S. C., Hines, D. C., Blaylock, M., Priddey, R. S., Brandt, W. N., & Egami, E. E. 2007, ApJ, 665, 157
Ganguly, R., Bond, N. A., Charlton, J. C., Eracleous, M., Brandt, W. N., & Churchill, C. W. 2001, ApJ, 549, 133
Ganguly, R., & Brotherton, M. S. 2007, ApJ, in press, arXiv: 0710.0588
Ganguly, R., Brotherton, M. S., Cales, S., Scoggins, B., Shang, Z., & Vestergaard, M. 2007, ApJ, 665, 990
Ghosh, K. K., & Punsly, B. 2007, ApJ, 661, L139
Hall, P. B., et al. 2002, ApJS, 141, 267
Hamann, F., Korista, K. T., & Morris, S. L. 1993, ApJ, 415, 541
Hewett, P. C., & Foltz, C. B. 2003, AJ, 125, 1784
Hopkins, P. F., et al. 2004, AJ, 128, 1112
Landy, S. D., & Szalay, A. S. 1993, ApJ, 412, 64
Murray, N., Chiang, J., Grossman, S. A., & Voit, G. M. 1995, ApJ, 451, 498
Ogle, P. M., Cohen, M. H., Miller, J. S., Tran, H. D., Goodrich, R. W., & Martel, A. R. 1999, ApJS, 125, 1
Pei, Y. C. 1992, ApJ, 395, 130
Proga, D., Stone, J. M., & Kallman, T. R. 2000, ApJ, 543, 686
Proga, D. 2007, ApJ, 661, 693
Reichard, T. A., et al. 2003a, AJ, 125, 1711
Reichard, T. A., et al. 2003b, AJ, 126, 2594
Richards, G. T., et al. 2002, AJ, 123, 2945
Richards, G. T., et al. 2006, AJ, 131, 2766
Schneider, D. P., et al. 2007, AJ, 134, 102
Shen, Y., et al. 2007a, AJ, 133, 2222
Shen, Y., et al. 2007b, ApJ, submitted, arXiv: 0709.3098
Skrutskie, M. F., et al. 2006, AJ, 131, 1163
Spergel, D. N., et al. 2007, ApJS, 170, 377
Stoughton, C., et al. 2002, AJ, 123, 485 (EDR)
Tolea, A., Krolik, J. H., & Tsvetanov, Z. 2002, ApJ, 578, L31
Trump, J.R. et al. 2006, ApJS, 165, 1
Vanden Berk, D. E., et al. 2001, AJ, 122, 549
Vanden Berk, D. E., et al. 2007, AJ, submitted
Vestergaard, M. 2003, ApJ, 599, 116
Weymann, R. J., Morris, S. L., Foltz, C. B., & Hewett, P. C. 1991, ApJ, 373, 23
Weymann, R. J. 2002, in Mass Outflow in Active Galactic Nuclei: New Perspectives, ed. D. M. Crenshaw, S. B. Kraemer, & I. M. George (San Francisco: ASP), 329
York, D. G., et al. 2000, AJ, 120, 1579
Zhou, H., Wang, T., Wang, H., Wang, J., Yuan, W., & Lu, Y. 2006, ApJ, 639, 716